ELSEVIER

Clinical Neurophysiology 119 (2008) 446–458

www.elsevier.com/locate/clinph

Quantification and visualisation of differences between two motor tasks based on energy density maps for brain–computer interface applications

A. Vuckovic [a,*], F. Sepulveda [b]

[a] *Centre for Rehabilitation Engineering, Department of Mechanical Engineering, University of Glasgow, James Watt Building (South) G12 8QQ, Glasgow, UK*

[b] *Brain–Computer Interface Group, Department of Computer Science, University of Essex, UK*

Accepted 18 October 2007

Abstract

Objective: To determine the most discriminative features for a brain–computer interface (BCI) system based on statistically significant differences between two energy density maps calculated from EEG signals during two different motor tasks.

Methods: EEG was recorded in ten healthy volunteers while performing different cue based, 3 s sustained, real and imaginary right hand movements. Energy density maps were calculated over fixed 240 ms and 2 Hz time–frequency windows (called resels) for each movement and statistically significant resels were determined. After that, normalised energy values of the statistically significant resels were compared between two real as well as between two imaginary movements using a parametric test.

Results: The largest differences between energy density maps between two motor tasks were noticed on electrode location Cp3 in the higher alpha and the beta bands (i.e., 12–30 Hz), for both real and imaginary movements. The method reduced a total number of discriminative features between two motor tasks to fewer than 2% for the imaginary and fewer than 3% for the real movements on the electrode location Cp3.

Conclusions: The method can be used for visualisation and feature extraction for BCI and other applications where event related desynchronisation/synchronisation (ERD/ERS) maps should be compared.

Significance: If a reliable on-line classification of imaginary movements of the same limb would be achieved it could be combined with classification of movements of different parts of the body. That would increase a number of separable classes of a BCI system, thereby providing a larger number of command signals to control the external devises such as computers and robotic devices.

Keywords: BCI; Energy density map; ERD/ERS; EEG; Motor task; Mental tasks

1. Introduction

Brain–computer interface (BCI) provides a novel communication channel between a person and its environment by recording brain signals and translating it into command signals to the external devices (Wolpaw et al., 2002). Therefore BCI is primarily designed to help patients with complete or severe damage of sensory-motor pathways to control objects in their surroundings like computers, wheelchairs and other assistive devices (Wolpaw et al., 2002). BCI systems rely on different internally or externally paced events (asynchronous or synchronous) and are often based on mental tasks like counting, mental rotation of object or imagination of motor tasks (Curran et al., 2004). A BCI discriminates between these different mental tasks and converts them into different commands. Performing the mental tasks results in changes in event related potential (ERP) and in oscillatory brain activity, that can be characterised

* Corresponding author. Tel.: +44 0 141 330 3251, +44 0 7906 441955; fax: +44 0 141 330 4343.

E-mail address: a.vuckovic@eng.gla.ac.uk (A. Vuckovic).

1388-2457/$32.00
doi:10.1016/j.clinph.2007.10.015

by event related desynchronisation and synchronisation (ERD/ERS) (Pfurtscheller and Lopes da Silva, 1999). One of the most frequently used tasks for the BCI systems is a motor task, i.e. imagination of movements of different parts of the body (Kauhanen et al., 2006; Vidaurre et al., 2006; Townsend et al., 2006). In addition, as a part of BCI studies, real movements of healthy persons are sometimes analysed and compared with the imaginary movements (Blankertz et al., 2006). During sensory-motor processing of the real or imaginary motor tasks ERD/ERS shows characteristic spatio-temporal patterns (Pfurtscheller, 1999; Neuper et al., 2006) that are similar for real and imagined movements (Leocani et al., 1999; Pfurtscheller and Neuper, 2001). In addition, these patterns show consistent variation between different frequency bands (Crone et al., 1998a; Crone et al., 1998b; Neuper et al., 2006). A classical approach for quantification and visualisation of ERD/ERS is to calculate and display ERD/ERS time courses, representing band power changes in specific frequency bands (Pfurtscheller and Aranibar, 1977; Pfurtscheller, 1999). Alternatively, a joint time–frequency approach can be used to provide a comprehensive overview of relative band power changes over broad frequency ranges (Makeig, 1993; Tallon-Baudry and Bertrand, 1999; Durka et al., 2001). Smaller time and frequency windows give a better resolution and help to precisely determine the most reactive regions but they also increase the possibility of detecting noise instead of relevant brain activity (Durka, 2006). Therefore, several methods have been proposed to find significant ERD/ERS regions, based on bootstrapping (Graimann et al., 2002, 2006) or normalisation and subsequent application of parametric tests (Zygierewicz et al., 2005; Durka, 2006).

However, a task of a BCI system is not only to detect the onset of significant changes in the oscillatory brain activity but also to separate between different motor tasks. In case of discrimination between movements of different limbs, differences in spatial and temporal distribution between significant ERD/ERS of two different movements can be quite obvious and can easily be visualised. In case of different movements of the same limb, there is very little variation in spatial distribution between ERD/ERS of different tasks, especially if the brain activity is recorded with surface recording methods, such as EEG or MEC.

Although from direct brain recordings it is known that real (Georgopolos et al., 1982; Kakei et al., 1999) or even imaginary movements in different directions (Lebedev et al., 2005) activate different populations of neurons, which can be at different distances from the recording electrode, it is questionable if these differences can be detected using a scalp EEG. Still, for each type of movement it is possible to calculate its own map of significant ERD/ERS changes in the time–frequency domain. Therefore an important issue for a BCI would be to visualise and quantify regions of the largest differences between significant ERD/ERS changes in two or more tasks.

In this paper, a method to compare statistically significant differences between two motor tasks, performed by the same hand, based on energy–density maps in fine time–frequency bands (240 ms and 2 Hz) is proposed. The method allows visualisation and quantification of differences between two energy density maps. Quantification of differences between two motor tasks would be useful to find the best features to automatically discriminate between these two tasks, in BCI applications based on motor or some other event related task. The efficacy of the method was demonstrated on both real and imaginary movements. The proposed method can be used for applications other than BCI, to compare between two ERD/ERS maps in general.

2. Methods

2.1. The experimental procedure

Ten neurologically healthy volunteers (8 men and 2 women, mean age 27.3 ± 7.8) participated in the study. All subjects signed a consent form based on the University of Essex's Ethical Committee recommendations. Subjects were comfortably seated in an armchair, their nose tips approximately 1 m from the computer screen, with the forearms on the armrest. They were asked to perform four types of real and kinaesthetic imaginary (i.e., the subject feels his/her limb executing a given action without visualising the movement) right wrist movements that would correspond to rotation of the wrist around two axes: extension (E)/flexion (F), and pronation (palm down P)/supination (palm up S). For practice, prior to starting to record the EEG, the subjects had one full training session (approximately 12 min) of real movements and half of a session of the imaginary movements. During the experiment, real and imaginary movements were separated in different sessions. Each subject performed three sessions of real movements and four sessions of imaginary movements in the following order: real, imaginary, real, imaginary, real, imaginary, imaginary. Each session consisted of 15 repetitions of four different movements (E, F, P and S, in random order), 60 movements in total. Hence, each subject performed 180 real and 240 imaginary movements. Each session lasted about 12 min and the break between the sessions was between 5 and 15 min to allow the subject to rest.

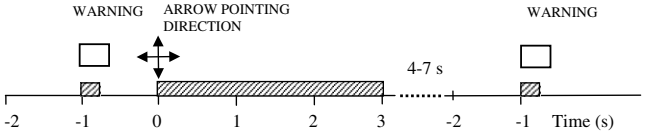

Fig. 1. Imagination protocol. A warning sign was presented 1 s before an arrow that indicated the type of movement, and stayed for 0.25 s on the screen. The arrow appeared at $t = 0$ s and stayed until $t = 3$ s. A subject was asked to perform a sustained movement while the arrow was on the screen. Meaning of the arrow directions: right = extension, left = flexion, up= supination, and down= pronation.

At $t = 0$ s a blank screen was presented to the subject (Fig. 1). At $t = 1$ s a warning sign (a rectangle) appeared for 0.25 s on the screen. At $t = 2$ s, an arrow of 5-cm length, pointing right (E), left (F), up (P) or down (S) stayed on the screen for 3 s, i.e., until $t = 5$ s. The arrow indicated the movement to be executed (letters in parentheses above). A subject was asked to perform a movement upon appearance of an arrow on the screen and to keep the hand in the required position, i.e., to perform a sustained movement, whether real or imagined, for all 3 s. After the arrow disappeared from the screen, the subject made a (non-sustained) movement to return the hand to the resting position. The time between the arrow's disappearance and the new warning was random between 4 and 7 s. The total time between two trials was between 9 and 12 s.

2.2. Data recording

The electroencephalogram was recorded using a 64 channel Biosemi™ ActiveTwo system with a sampling frequency of 256 samples/s. Electrode placement was done according to the Biosemi ABC system, which, for 64 electrodes, corresponds to the international 10–10 system (ACNS, 2006). The ActiveTwo System has a preamplifier stage on the electrode and can correct for high impedances (in the range of 100 kOhm), so impedance measurements are not necessary (MettingVanRijn et al., 1990). In order for the correction to be effective, the offset voltage (between the A/D box and the body) was verified to be within 50 μV, the range recommended by Biosemi, The Netherlands (Biosemi ActiveTwo System, 2007), during electrode placement and with no blinking artefacts. To prevent saturation of the signal during EOG artefacts, the BioSemi ActiveTwo system has a dynamic adjustable range and can record EMG and EEG on all electrodes. The system has eight additional monopolar electrodes (called EX here) for measuring potentials from the other parts of the body. The reference electrode for EEG recording was an EX electrode placed on the right ear. All electrodes had the same ground. Electro-oculograms (EOGs) were recorded from the *orbicularis oculi*, from the outer cantus of the right eye, and below the right eye. Simultaneously, forearm EMG was bipolarly recorded during real and imaginary movement with two pairs of EX electrodes placed 2 cm apart on the *flexor carpi* and *extensor carpi* (Hermens and Freriks, 1999a). Thus, it was possible to determine whether there was any real movement during imaginary movement sessions. Also, to detect the onset of muscle activity, EMG was rectified and averaged over 30 ms (Hermens and Freriks, 1999b). The criterion for movement onset was that the averaged EMG (while the arrow was on the screen) exceeded mean ± (2*SD) of the averaged EMG from the first 50 ms of the reference period (the reference period started 1 s before the warning sign, which had no muscle activity related to the analysed movement).

2.3. EOG removal using independent component analysis

EOG artefact was minimised using independent component analysis (ICA) as described in Onton and Makeig (2006). ICA components containing EOG artefacts were determined by comparing the ICA components with the EOG recordings and by checking the spatial localisation of the components. Components that included the strongest EOG (blinking artefacts) were set to zero before inverting the data to the EEG domain. It was possible that some EOG still remained after EOG removal, but that would affect mainly lower EEG frequencies (0–2 Hz). In addition, the signal was averaged and statistically significant differences between two energy maps were calculated. Therefore, the influence of the remaining EOG should be negligible because it was unlikely that the EOG that remained after EOG removal and averaging of the signal was biased towards one type of movement.

2.4. Data pre-processing

The raw EEG was referenced to the right ear and filtered (Butterworth filter of the 5th order, zero lag, high pass cut off frequency at 0.5 Hz and low pass cut off frequency at 100 Hz). In addition, a Butterworth stop-band filter was applied at 50 Hz. To obtain a reference-free recording, a Laplacian that included the centre and the four nearest electrodes (three nearest electrodes for electrodes at the edge) was calculated (Hjort, 1975). The EEG signal was visually inspected and poor quality EEG segments were removed. The exclusion criterion was that the amplitude of the spurious signal exceeded three times the standard deviation of the EEG amplitude (Talsma and Woldorff, 2005). That left 35–40 real movement trials (out of 45) and 50–55 imaginary movement trials (out of 60) for each type, for each subject.

2.5. Time–frequency analysis

The Discrete Gabor transformation was applied to the EEG signal to calculate the Gabor coefficients (GCs). The Gabor transformation is a windowed Fourier transformation with a fixed size of the windows in both time and frequency (Qian and Chen, 1996; Munk, 2000). To calculate Gabor coefficients, the temporal resolution was 120 ms and the frequency resolution was 2 Hz.

The windowing function used was the Gaussian function. In this study, only a direct DGT was applied to calculate the Gabor coefficients, as follows:

$$\mathrm{GC}_{mn} = \sum_{k=0}^{L-1} S[k] \cdot \gamma[k - m \cdot \Delta M] \exp\left(-jkn\frac{2\pi}{N}\right), \quad -\Delta N < m < \Delta N \quad 0 \leqslant n \leqslant \Delta M - 1 \tag{1}$$

$$\gamma[k] = \sqrt{\frac{\sqrt{2}}{T_1}} \cdot \mathrm{e}^{-\pi \cdot \left(\frac{k-0.5(N_1-1)}{T_1}\right)^2} \quad 0 \leqslant k \leqslant N_1 - 1,$$

$$T_1 = \sqrt{\Delta M \cdot N},$$

where S is EEG signal, γ is the analysis Gaussian function, $N_1 = 256$ is the number of samples in the analysis function (and at the same time it is the number of grid points in the time and frequency dimension), $\Delta M = 32$ is the time step, $\Delta N = 2$ is the frequency step, i.e., the bandwidth, $N = 128$ is the number of frequency steps ΔN in the frequency dimension and L is the total number of samples in the analysed 6 s epoch (Munk, 2000). Only GCs corresponding to 0.5–100 Hz (50 frequency bands, width of each band 2 Hz) were included for further analysis. In that way the δ, θ, α, β and γ ranges were taken into account.

The energy for each time–frequency window was calculated as:

$$E_{mn} = (\mathrm{abs}(\mathrm{GC}_{mn}))^2 \tag{2}$$

and the energy for two adjacent time windows was averaged, thus giving energy values for time–frequency windows of 2 Hz by 240 ms. This was done as suggested in Durka (2006); Zygierewicz et al. (2005) to reduce detection of "noise". These time–frequency windows were called "resels" (Durka, 2006; Zygierewicz et al., 2005).

2.6. Calculating ERD/ERS and their statistical significance

The ERD/ERS maps of statistically significant resels were calculated following a procedure described in Zygierewicz et al. (2005):

- The energy values for each resel were normalised using a Box–Cox transformation (Box and Cox, 1964), giving E^{norm}_{mn}, where m is a given frequency band and n is a given time window.
- A paired t-test was performed between energy levels of a reference period in the frequency band m and energy values of each resel in the period after the cue onset E^{norm}_{Mn}, in the corresponding frequency band. The significance level for the t-test was 0.05.
- A method to estimate the false discovery rate (significance level 0.05) was applied to reduce the number of falsely detected noisy resels (Benjamin and Yekuteli, 2001).
- For the chosen resels, ERD/ERS maps were calculated based on non-normalised values:

$$\mathrm{ERD/ERS}(m,n) = \frac{\overline{E(m,n)} - \overline{E_{\mathrm{ref}}(m)}}{\overline{E_{\mathrm{ref}}(m)}}. \tag{3}$$

For each subject, the time–frequency distribution of the ERD/ERS responses was determined and the electrode location of the strongest ERD/ERS response was defined. The reference period was from 2640 ms to 1640 ms before the cue onset (values determined by the time resolution for calculating the Gabor coefficients) and the time–frequency windows were 240 ms by 2 Hz.

2.7. Comparing energy levels for two different conditions

To compare energy levels between two different energy density maps it was necessary to find resels with statistically significant energy changes for both maps. In general, these two maps were made based on unequal numbers of single trials K_1 and K_2. Therefore to find which resels have statistically significant difference for energy levels between the two conditions, an unpaired t-test was applied for each of the corresponding resels and H and p values were obtained as follows:

$$[H_{m,n}, p_{m,n}] = t\text{-test}\left(E1^{\mathrm{norm}}_{m,n}, E2^{\mathrm{norm}}_{m,n}\right) \tag{4}$$

In this way, new maps containing H or p values for each resel were obtained. H maps contained the values 0 (non-significant) or 1 (significant) for each resel. P maps contained p values for each significant resels. For all resels that had $H = 0$, the value of p was set to 1.

To account for false detection of significant resels due to multiple comparison, a method for false discovery rate (FDR) estimation (Benjamin and Yekuteli, 2001) was applied again, with a significance level of 0.05.

The proposed method was implemented on data for each single subject, for both real and imaginary movements. H and p maps of statistically significant differences between any combination of two movements (extension–flexion EF, extension–supination ES, extension–pronation EP, flexion–supination FS, flexion–pronation FP, supination–pronation SP) were calculated for each single subject. Grand average maps of H values were obtained as well and were compared with the H maps of the single subjects. To illustrate differences between H values for each single subject and the grand average values, the H maps for two single subjects are shown in the next section. H and p maps were calculated for a period lasting 6 s that started 3 s before the cue (arrow) onset and ended 3 s after the cue onset, when the cue disappeared from the screen. A sustained movement was performed in the last 3 s of that 6-s period.

3. Results

3.1. ERD/ERS maps

The ERD and ERS maps showed regions of desynchronisation and synchronisation in nine out of ten subjects. In one subject, clearly defined ERD/ERS regions could not be detected so the subject was excluded from further analysis. Alpha frequency range desynchronisation (8–14 Hz) was noticed in the remaining nine subjects in the sensory-motor region (corresponding to location of C, Cp and CF electrodes). Meta desynchronisation was also noticed in the same region in four subjects for the imaginary movements and in five subjects for the real movements. In three subjects delta ERD was noticed for the imaginary movements. In two subjects there was an

ERS in the frequency range above 40 Hz. Although the ERD/ERS maps were calculated for the 0.5–100 Hz frequency range, resels with a statistically significant ERD/ERS were not clustering for the higher frequencies and it was not possible to exclude the possibility that they represented noise. Therefore, only frequencies up to 60 Hz are shown in the results.

The strongest ERD/ERS responses were detected in regions that corresponded to electrode locations CP3 and C3 for both real and imaginary movements. The location with the strongest ERD/ERS responses typically remained the same for all four types of movements for each subject. Dominant frequencies were in most cases the same for all four types of movements for a single subject, but their temporal distribution differed among the movements. These dominant frequencies were in the alpha frequency range (8–14 Hz) in all subjects and in five subjects in the beta range (up to 30 Hz). In most cases, for a single subject, the location of the strongest ERD/ERS responses remained the same for the real and the imaginary movements and

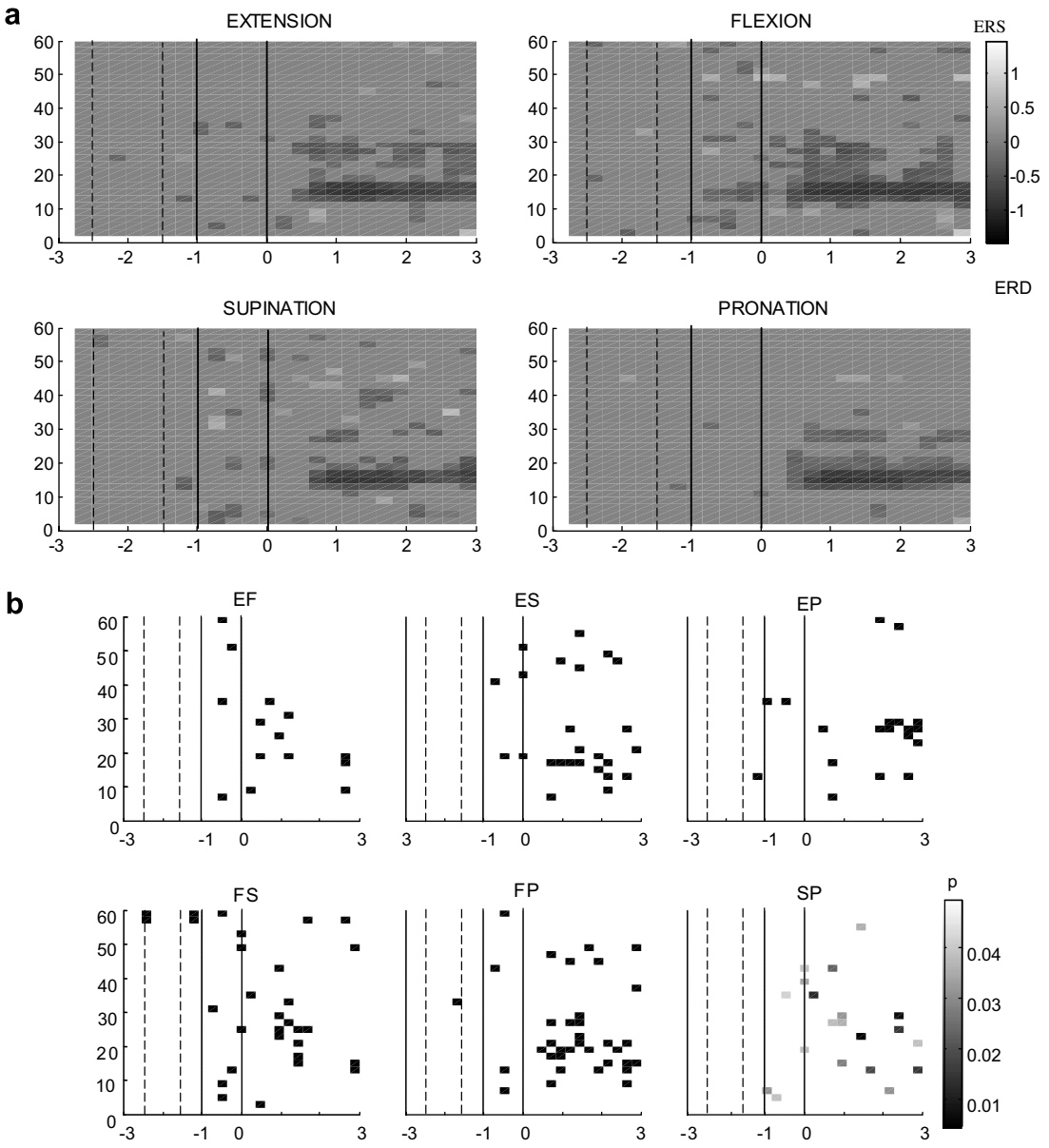

Fig. 2. (a) Time–frequency maps of statistically significant ERD/ERS for four different types of real movements on electrode CP3 of one subject. A 1-s long reference period is marked by the vertical dashed lines. At $t = -1$ s (the first solid line from left) a warning sign was shown on the screen. A cue (an arrow) appeared on the screen at $t = 0$ s (marked with the second vertical solid line) and stayed for 3 s until $t = 3$ s. (b) Time–frequency H maps showing regions of statistically significant differences between two ERD/ERS maps. Each of the six H maps was calculated for one combination of two (out of four) ERD/ERS maps shown in Fig. 2a. The lower left map shows a p map instead of a H map to demonstrate the different significance levels in different resels (all of these resels were statistically significant, i.e., they had $H = 1$). EF, extension–flexion; ES, extension–supination; EP, extension–pronation; FS, flexion–pronation; FP, extension–pronation; SP, supination–pronation.

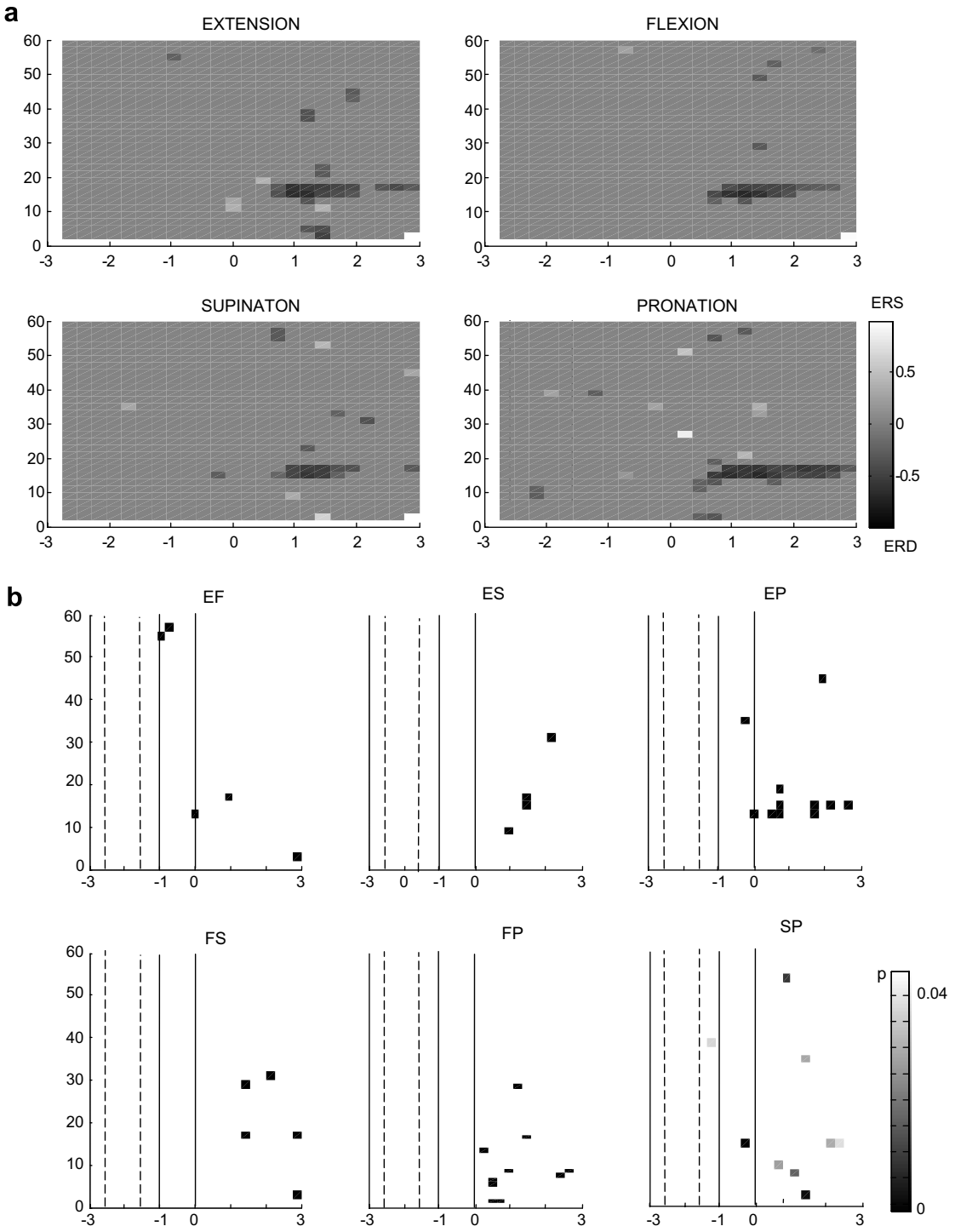

Fig. 3. (a) Time–frequency maps of statistically significant ERD/ERS for four different types of imaginary movement on electrode CP3 of one subject. A 1-s long reference period is marked by the vertical dashed lines. At $t = -1$ s (the first solid line from left) a warning sign was shown on the screen. A cue (an arrow) appeared on the screen at $t = 0$ s (marked with the second vertical solid line) and stayed for 3 s until $t = 3$ s. (b) Time–frequency H maps showing regions of statistically significant differences between two ERD/ERS maps. Each of the six H maps was calculated for one combination of two (out of four) ERD/ERS maps shown in (a). The lower left map shows a p map instead of a H map, to demonstrate the different significance levels of different resels (all of these resels were statistically significant, i.e., they had $H = 1$). EF, extension–flexion; ES, extension–supination; EP, extension–pronation; FS, flexion–pronation; FP, extension–pronation; SP, supination–pronation.

corresponded to either C3 or CP3 electrode location. However, the location of the strongest ERD/ERS responses was in two cases on the CP3 for the imaginary and on the C3 for the real movements.

Fig. 2a shows ERD/ERS maps for four real movements for one subject for electrode location CP3. Fig. 3a shows ERD/ERS maps for imagination of the same four types of movements, on the same electrode location of the same

subject. The ERD was stronger for the real than for the imaginary movements, by up to 75%, and spread over a 2–4 Hz wider frequency bands, in the alpha and the lower beta frequency range. The frequency range of the ERD (higher alpha and beta) was similar but was wider for the real (12–30 Hz) than for the imaginary (14–18 Hz) movements. In addition, for the real movements an ERD can also be noticed in the frequency ranges up to 40 Hz. The ERS lasted up to 0.5 s and was mostly restricted to isolated 2 Hz bands. The ERS was up to 75% of the ERD.

3.2. Detection of statistically significant differences in energy levels between two types of movements

Fig. 2b shows regions with statistically significant differences between two types of real movements (supination and pronation) on the electrode location CP3. All figures apart from the lower right one show H maps and the last one shows a p map. H maps, which are binary, are presented because of their better legibility compared to the gray scales in p maps. A p map is shown for one case only to demonstrate significance levels of differences between resels of two ERD/ERS maps. H maps were calculated for all six possible combinations of four movements (EF, ES, EP, FS, FP, SP). H maps shown in Fig. 2b were calculated for 6 s long periods. The period started at $t = -3$ s, that is, 3 s before the cue onset (the cue onset was at $t = 0$ s), and finished when the cue disappeared from the screen (at $t = 3$ s). A sustained movement was performed during the last 3 s, while the cue was on the screen.

For an EF (i.e. extension/flexion) combination, most of the resels were in the lower beta range in the first second after the cue. From Fig. 2a it can be noticed that extension and flexion energy maps have the largest differences in the beta frequency range during the first second. For the ES combination, significant resels clustered in the beta (14–30 Hz) and the lower gamma range (44–56 Hz). From Fig. 2a it can be seen that an ERD for flexion starts 240 ms earlier than a ERD for supination (figure labelled with FS). Therefore, the H map shows differences in energy levels in frequency band 16–18 Hz during almost 1 s. Similar differences can be noticed for the other combinations of movements. Fig. 3b shows H maps for imaginary movements of the same person and on the same electrode location. The number of significant resels was smaller in the case of the real movements and could not be easily compared with the corresponding ERD/ERS maps. Similar to the real movements, different types of movements have different delays for the start of significant ERD. This shows that the afferent feedback (absent in the case of imaginary movements) was not the only cause for the different temporal distribution of significant ERD/ERS resels for different types of movements. Only in the case of an H map obtained for the EP combination it can be noticed that significant resels clustered in the 14–18 Hz range that corresponded to differences of the ERD/ERS maps of extension and pronation (Fig. 3a).

It can also be noticed that some significant resels were falsely detected in the reference period and in the period between the warning and the cue. These resels have been falsely detected in the process of determining regions with significant energy changes for each type of movements. For example, two resels on 60 Hz in extension ERD/ERS map, in the reference period (Fig. 3a), are found significant on the H map of EF (Fig. 3b). However, the rest of "noise" resels from the ERD/ERS maps on the same figure are not marked as significant. Although there are statistically significant resels in the energy density maps for each movement between warning sign and a cue, which probably indicates expectation (e.g., ERD in the alpha range in Fig. 2a, flexion), it is not likely that statistically significant resels before the cue (in the H map) have a physiological origin, because the order of movements was random.

A way to reduce the number of falsely detected resels would be to look at p instead of H maps as they show the significance levels for different resels. From the lower right figures in Figs. 2b and 3 it can be noticed that most of the "noise" resels in the period before the cue had lower significance levels, i.e. larger p values, compared to the resels after the cue.

Fig. 4 shows one more example of a topographic display of a H map for significant differences between two real movements, extension and pronation, for one more single subject, in the sensory-motor region. The largest number of significant resels was on electrode location CP3 and in general in the centro-parietal area, on both the contra (left) and the ipsilateral (right) side.

The time–frequency distribution of H maps for a certain combination of movements was not homogeneous for all subjects. Therefore, a general analysis of differences between H maps for different combinations of movements was not performed in this study. Such analysis would probably require a larger number of subjects though it is questionable if such subtle differences could be recorded with EEG.

Table 1 shows the number of significant resels as a percentage of the total number of resels (in frequency range 0–60 Hz and in the time interval 0–3 s) for all six combinations of imaginary and real movements, on the electrode location CP3. The number of significant resels was in average less than 2% for the imaginary and less than 3% for the real movements. This shows that the method was also efficient for feature selection in a BCI system, but choice of the best (i.e. the most discriminative) features can be further refined by subsequently applying some other method for feature extraction to additionally reduce the number of the resels, i.e. features.

Besides finding the most discriminative features in the time–frequency domain on each electrode site, the most discriminative recording sites can be determined as well. To determine general most discriminative sites, grand average H maps were made.

Fig. 5 shows a topographic display of a grand average H map over nine subjects for discrimination between two real

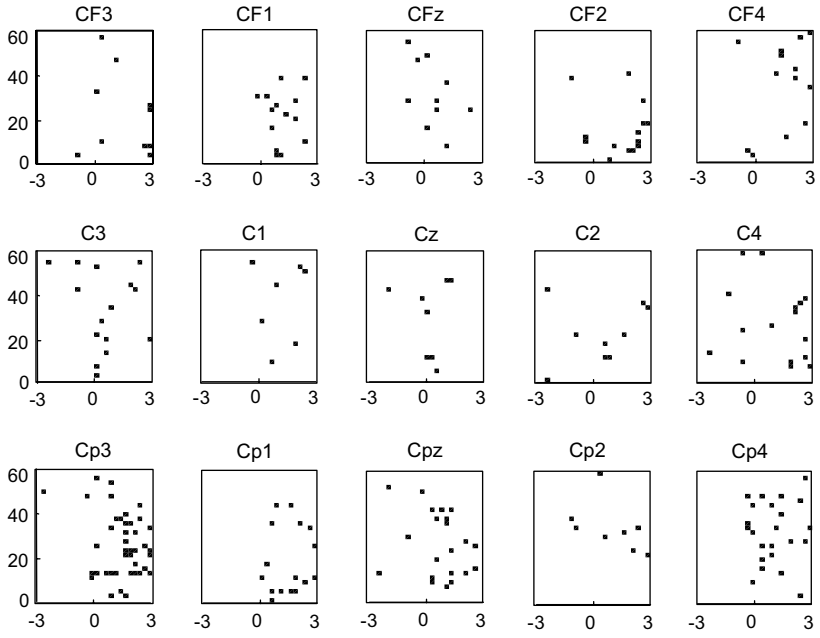

Fig. 4. A topographic presentation of time–frequency H maps for real movements (extension vs. pronation) for one subject, in the sensory-motor region. The time–frequency distribution of statistically significant changes of energy levels on each electrode for each movement was calculated first. After that, the H maps of statistically significant differences between energy level maps were calculated for each electrode. Frequency range was 0–60 Hz and time window was from $t = -3$ s to $t = 3$ s.

Table 1
The average number (in percentage) of resels which show statistically significant difference between two motor tasks for imaginary and real movements, on electrode location CP3

	E–F	E–S	E–P	F–S	F–P	S–P
Imaginary	1.2 ± 0.5	1.3 ± 0.5	1.3 ± 0.5	1.4 ± 0.6	1.6 ± 1.1	1.8 ± 0.9
Real	2.7 ± 1.1	1.6 ± 0.5	1.4 ± 0.9	1.6 ± 0.5	2.9 ± 2.9	2.0 ± 0.9

EF, extension–flexion; ES, extension–supination; EP, extension–pronation; FS, flexion–pronation; FP, extension–pronation; SP, supination–pronation.

movements, supination and pronation, in the sensory-motor region. The darker colour means that the resel was found significant in more subjects. For example, a level of $1/9 = 0.11$ on the colour bar means that the resel was found significant in one person while a level 0.44 means that it was significant in four out of nine subjects. The resels were distributed over the whole 3 s during sustained movements. The most discriminative region corresponded to a location of the electrode CP3 (12–30 Hz) and ipsilaterally (on the right) to location of the electrodes C4 and CP2 (14–18 Hz). A region with a lot of discriminative resels was also in the frontal part on both contra (left) and ipsilateral (right) side and parietally on the electrode location P2 (12–30 Hz) on the ipsilateral (right) side. In the frontal region, the most discriminative resels were found in the lower beta range (14–18 Hz) on electrode locations F1 and F2 and also in the delta range (0–4 Hz) on electrode locations F1, Fz, F2 and F4. There were also some sparsely distributed resels over the whole 0.5–60 Hz range.

Fig. 6 shows a topographic display of the grand average H map over the same nine subjects, for the same type of movements (supination), but imagined instead of executed. It was not possible to visually determine any particular region with the largest number of discriminative resels (although a region corresponding to the electrode location CP3 had the strongest ERD/ERS in most of cases). It can be noticed that some narrow frequency bands, belonging to the higher alpha and the lower beta band, marked with asterisks (C3, 14–16 Hz; CF5, 10–12 Hz; CP2, 10–12 Hz), were discriminative in continuity for 1.5 s. Many significant resels belonged to the delta range, especially in the frontal region (corresponding to electrode locations F3 and F2). As described previously in Section 2 for removing EOG artefact, it was not likely that the delta activity (especially in 2–4 Hz range) reflected eye-movement artefacts, but it cannot be ruled out that it represented some other mental process other than kinaesthetic movement imagination, such as visual imagination (Neuper et al., 2005) or visual processing of cues, i.e., arrows pointing in different directions shown on the screen (Hopf and Mangum, 2000).

Fig. 7 shows the grand average H map for all six combinations of the real movements on the electrode location CP3. Most of the statistically significant resels were witnessed in the 12–30 Hz frequency range. Clustering of significant resels could be noticed for all combinations of movements but was the most pronounced for EP, SP and FP. However, the result for the grand average was not directly transferable to each individual subject, which can

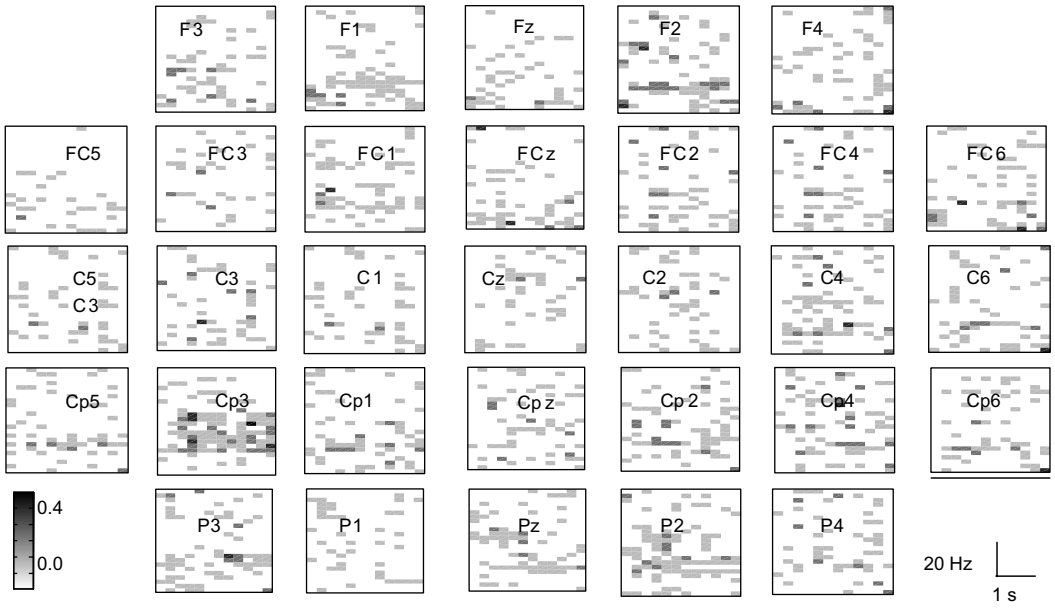

Fig. 5. Grand average time–frequency H map for statistically significant differences between right hand supination and pronation (real movements). Only the 3 s after the cue onset are shown. The frequency range was 0.5–60 Hz.

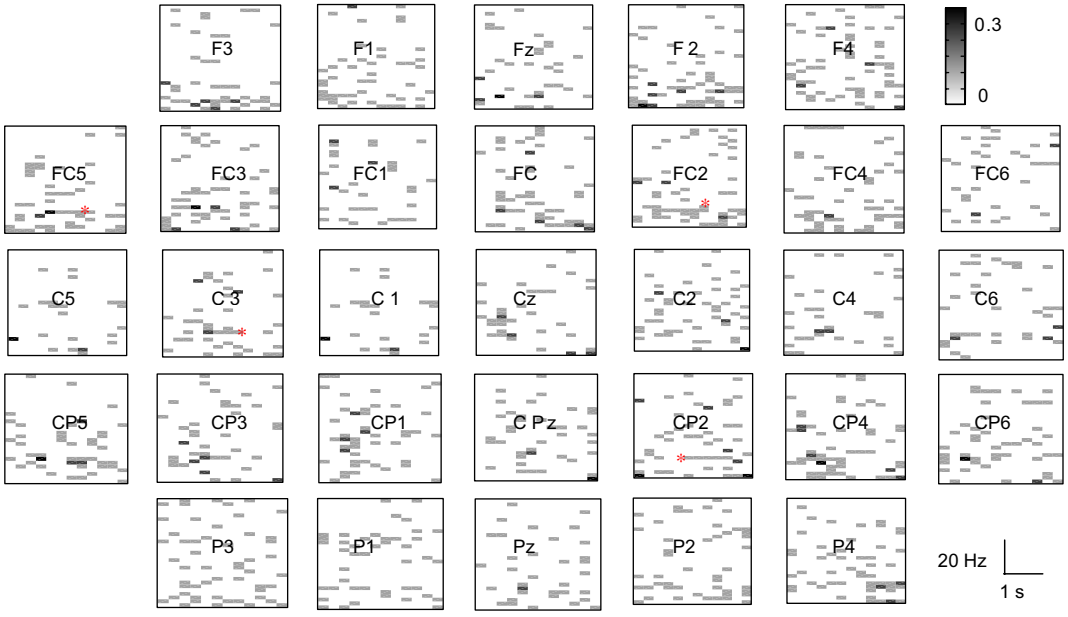

Fig. 6. Grand average time–frequency H map for statistically significant differences between right hand supination and pronation (imaginary movements). Asterisks indicate 2 Hz frequency bands that show activity of 1 s or longer. Only the 3 s after the cue onset are shown (from $t = 0$ s to $t = 3$ s). The frequency range was 0.5–60 Hz.

be noticed by comparing Fig. 7 with Figs. 2 and 4. Although H maps were calculated for each single subject, because of complexity of the figures and large number of movement combinations, H maps were illustrated on the movements of two single subjects only.

Fig. 8 shows the grand average H map for all six combinations of the imaginary movements on the electrode location CP3. In contrast to the real movements, clustering of significant resels in the higher alpha and the lower beta range (12–20 Hz) was obvious only for FS and FP.

4. Discussion

BCI systems based on motor tasks often use features extracted from the ERD/ERS maps. In order to determine the most representative features various methods were proposed to determine regions of statistically significant ERD/ERS (Graimann et al., 2002; Zygierewicz et al., 2005). These methods basically show regions with the highest relative increase/decrease of energy in narrow frequency bands, during the motor task, compared to the reference

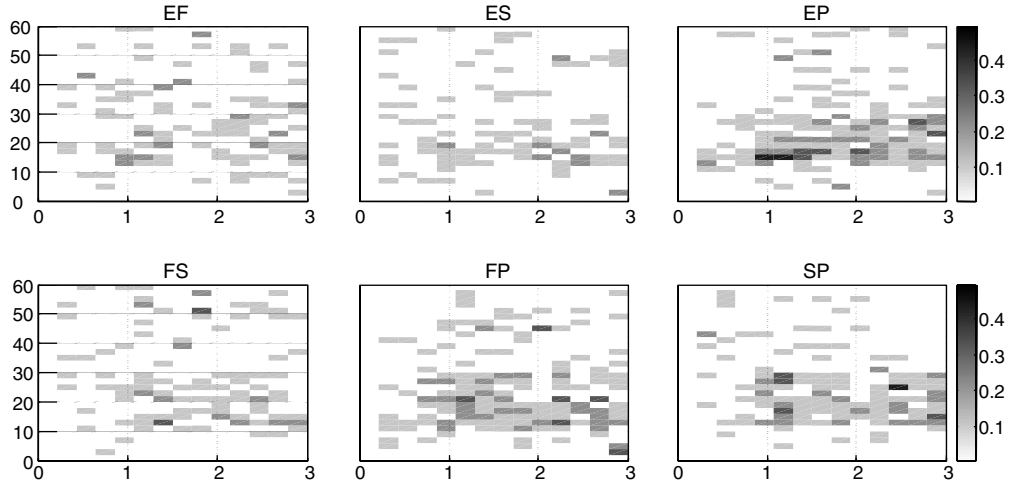

Fig. 7. Grand average time–frequency H map on electrode location CP3 for all six combinations of real movements. Only the 3 s after the cue onset are shown, from $t = 0$ s to $t = 3$ s). The frequency range was 0.5–60 Hz.

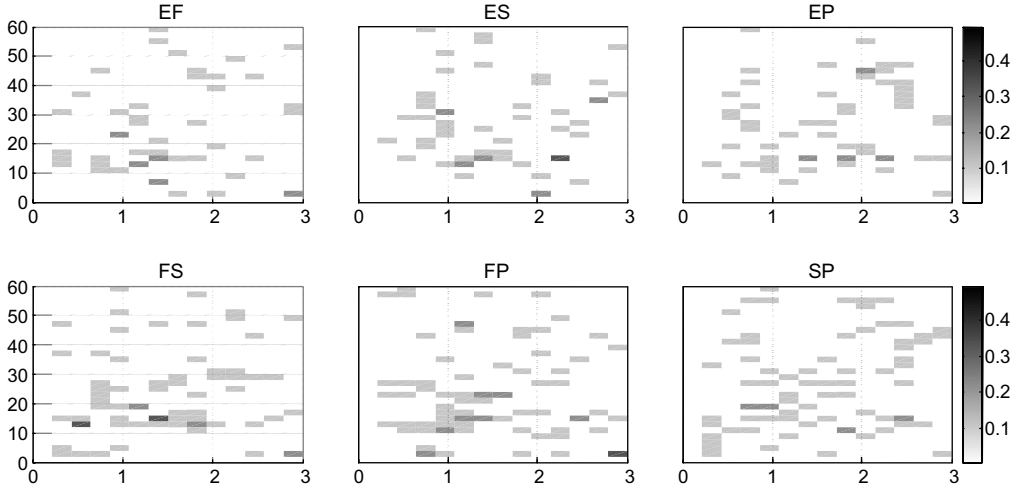

Fig. 8. Grand average time–frequency H map on electrode location CP3 for all six combinations of the imaginary movements. Only the 3 s after the cue onset are shown, from $t = 0$ s to $t = 3$ s). The frequency range was 0.5–60 Hz.

period, when there was no activity related to the task. However, BCI systems are often based on discrimination between different motor tasks. Therefore another important issue of the BCI would be to visualise and quantify, based on relative energy maps, regions in the time–frequency plane with the largest differences between the two maps. In ERD/ERS studies based on real movements of different parts of the body visualisation and quantification of these regions might not be very difficult due to differences in spatial distribution of two ERD/ERS maps. However if imaginary movements should be compared or if movements should be performed with the same part of the body regions of largest differences in ERD/ERS maps cannot be easily visually determined (Pfurtscheller et al., 1999).

This paper proposes a method to determine spatial, time and frequency regions of significant differences between two energy maps based on the EEG signal of individual subjects while they performed two different real or imaginary motor tasks with the same hand. The method represents an extension of a method proposed by Zygierewicz et al. (2005); Durka (2006) where energy density maps were calculated based on the Matching Pursuit algorithm (Mallat and Zhang, 1993). Matching Pursuit is a data driven method that allows determining optimum time–frequency windows. However, to calculate statistically significant differences in ERD/ERS maps, a finite size time–frequency window (250 ms by 2 Hz) was used in that study, which is similar to the time–frequency windows used in the present study (240 ms by 2 Hz).

The energy values were calculated based on the Gabor transformation, which is the only one way of calculating a time–frequency energy density, that can also be calculated using for instance, Fourier transformation, continuous wavelet transformation or matching pursuit. The only requirement is that the corresponding time–frequency

windows of two energy–density maps have the same size so that they can be compared.

The proposed method enabled calculation and visualisation of significant differences between two motor tasks even when these tasks activated the same region of the cortex and the difference in the ERD/ERS maps cannot be easily visually observed.

In addition to visualisation of regions with significant differences in energy density maps, the method can also be utilised to find the most discriminative features (resels) between the two motor tasks. A percentage of statistically significant features was on electrode location CP3, from $1.2 \pm 0.5\%$ to $1.8 \pm 0.9\%$ for the imaginary movements and from $1.4 \pm 0.9\%$ to $2.9 \pm 2.9\%$ for the imaginary movements. The method significantly reduced a total number of possible candidate features for a BCI classifier, acting as a feature selection. Selected features could be used as an input to a BCI classifier. In addition to reducing a number of features in the time–frequency plane, the method also determined spatial locations of regions with the largest differences between the two tasks. That could further reduce the number of necessary recording electrodes, which is a requirement for an on-line BCI system. The same method could be applied to visualise differences between imagination and execution of the same motor tasks.

The calculation of Gabor coefficients for single epochs followed by the calculation of statistically significant ERD/ERS took between 3 and 4 s (all programs executed in Matlab 7, on a PC Pentium with 1 GB RAM), which is less than the duration of an epoch (6 s) used in this study. In general, epochs for on-line BCI purposes last several seconds (e.g., one epoch lasted 7 s in (Vidaurre et al., 2006). Therefore, the feature extraction method proposed in this study, followed by feature classification, should be applicable for many on-line BCIs. EOG removal was not included in the estimation, because it was performed before calculating the Gabor coefficients. In real-time applications, two possible solutions could be tried: (a) to ignore EOG artefacts and avoid using EEG from the most frontal electrodes, or (b) to pre-calculate an ICA matrix containing only EOG components and then to apply that matrix to the new data on-line, assuming that the nature of EOG artefacts does not change over time.

In addition, because the analysed data's distribution has been normalised, it can also be applied for a multiclass comparison using ANOVA or similar tests. In examples shown in this paper, differences between the real movements could be easily visualised. For the imaginary movements, the number of significant resels was smaller than for the real movements. Therefore, it was not easy to visually determine the regions with the largest differences but as already mentioned due to the relatively small number of significant resels, they could be used (for each of two types of movements) as a feature input for a two class classifier.

Statistically significant ERD/ERS changes for single subjects showed different temporal distributions (up to 240 ms) in the same frequency range for different types of movements. These differences were noticed for both real and imaginary movements of the same person, showing that they were not caused only by afferent feedback. A possible explanation for different temporal distribution in statistically significant ERD/ERS changes for different types of movements could be that the maps represented only statistically significant ERD/ERS changes while slight ERD/ERS changes may have started earlier.

Although the method works well for the given application it has several limitations:

1. It can be used only if the two different tasks were performed during the same experiment (so that the electrode locations for the two tasks are the same). If maps obtained during two different sessions were to be compared, it would be a problem to determine whether the origin of the differences was due to different electrode locations or to the actual time variations between two sessions caused, for instance, by learning. However, this is a general problem related to EEG recordings and it is not restricted to our method only.
2. In this study it was assumed that the reference period was the same for both tasks. If that were not the case, it would be more appropriate to compare the whole energy maps instead of maps of resels showing significant differences compared to the reference period (personal communication with Dr. Zygeriewitz). The problem with comparing whole energy maps, instead of only significant parts therein, would be that the number of falsely detected significant resels would increase with the increase in the total number of resels that are simultaneously compared (Zygierewicz et al., 2005; Benjamin and Yekuteli, 2001).
3. In the present study, behavioural data were not monitored, though existence of such data could reduce trial to trial variance, because the existing reference point, an arrow on the screen could be replaced with some more reliable physiological measurement. The reason for this choice is that in BCI experimental paradigms, which are based on calculating ERD/ERS maps, it is not usual to provide behavioural control, especially because BCI experiments are often based on imaginary movements and other mental tasks that may not elicit measurable behavioural outputs. Even experiments on which methods for calculating significant ERD/ERS maps were demonstrated (e.g., Crone et al., 1998a; Graimann et al., 2002; Zygierewicz et al., 2005) have had no behavioural control. In addition the analysed time window of 240 ms was quite large and precisely defined reference point would not be of much use.
4. About 10% of population do not have clearly distinguishable brain states related to the motor imagery or execution (Pfurtscheller and Neuper, 2001). In the current study, in one out of ten subject there were no significant ERD/ERS changes and the proposed method could not be applied.

The method was not completely insensitive to noise and that sensitivity was due to the sensitivity of the method for finding significant ERD/ERS changes. A way to overcome this would be to avoid analysing very high frequencies and to look at p instead of H maps, so that the relative importance of each resel can be determined. However, this is not a straightforward solution because all resels in a H map are already statistically significant and setting a new p level would depend on the specific data set and the purpose of the analysis. Alternatively, depending on the purpose, different significance levels in a t-test can be used.

The results obtained in this study are in accordance with previous ERD/ERS studies (on imaginary and real movements) that showed the most significant changes in the alpha and beta ranges in the hand representations area (Pfurtscheller et al., 1999). On the other hand, the present study is not completely comparable with the previous ones because they either looked at ERD/ERS for different limbs or for different types of movements. In Pfurtscheller et al. (1999), differences in ERD/ERS during voluntary finger, thumb and wrist movements were analysed. Similarly to the current study, movements in these three parts of the body activated approximately the same region of the cortex. An ANOVA test was used to compare between ERD/ERS during and after movements in different parts of the hand (Pfurtscheller et al., 1999). The largest differences were found in the post-movement beta ERS. However, the method used in that study allowed only a rough separation into pre- and post-movement periods. Further, the ANOVA test was applied (without data normalisation) to data that in general do not have a normal distribution.

In the present study, the largest differences between the energy levels of two energy density maps were found in the higher alpha and the beta ranges (i.e., 12–30 Hz). However, a clear post-movement beta ERS was not noticed because only a 3-s period during a sustained movement was analysed. Analysis of the post-movement period was not possible because the 3 s sustained movement was followed by another movement to bring the hand back to the resting position (e.g., extension was followed by flexion and flexion was followed by extension). Therefore, if the post-movement period was included, both types of movement would be present in both cases.

The grand average map for the real movements showed that the CP3 location contained the largest amount of significantly different resels between two movements of the same (right) hand, independently of the movement type. However, it is interesting to note that there were quite a few significant resels on the ipsilateral (right) side, on electrode locations P2 and F2.

The grand average H map for imaginary movements did not clearly show that the CP3 location contained the largest number of significantly different resels, but, Fig. 8, presenting enlarged H maps on electrode location CP3 for all six combinations of imaginary movements, showed clustering of significant resels in the higher alpha and the lower beta range (12–20 Hz). The grand average H map also showed activity in the delta range in the frontal region, which might suggest that the subjects combined kinaesthetic and visual imagination. Neuper et al. (Neuper et al., 2005) showed that there is a difference between the spatial localisation of kinaesthetic and visual imagination, respectively, the former being mostly localised in the sensorymotor area and the latter being more widespread. In another BCI study, based on EEG and MEC recordings, tetraplegic patients were asked to attempt to perform left, right, or both index finger movements (Kauhanen et al., 2006). It is likely that patients in that study, who could not perform real movement for long periods of time, preferred visual imagination. In that study, the best classification accuracy was achieved with features in the 0.5–3 Hz range when brain signals were recorded bipolarly from F3–F4, C3–C4 and P3–P4. i.e., the best classification accuracy was achieved with features in the delta band and recorded not only from the central but also from frontal and parietal sites.

In a previous study of ours, the same data were used to classify between two different groups of imaginary movements and an average classification accuracy of 80% was achieved (Vuckovic and Sepulveda, 2006). Classification was based on neural networks and the input features were the absolute values of Gabor coefficients (in the 8–80 Hz frequency range) calculated on Independent Components rather than on the EEG signal, so precise localisation of most significant resels was not possible. Choosing the best features based on the proposed method would have advantages compared to the method based on the Independent Components because it would enable precise spatial location of significant features and could be used in on-line applications. Further, the number of independent components may vary over time and their on-line updating would add to the computational cost.

If a reliable on-line classification of imaginary movements of the same limb would be achieved it could be combined with classification of movements of different parts of the body. That would increase a number of separable classes of an BCI system, thereby providing a larger number of command signals to control the external devises such as computers and robotic devices.

This study was based on a motor task. However, ERD/ERS can be a result of many other events (Pfurtscheller and Lopes da Silva, 1999; Neubauer et al., 2006; Krause, 2006). The proposed method for finding significant features can also be used for discrimination of such tasks, whether used for BCI applications or not. It is not limited to the EEG recordings and could be applied to different methods of recording brain activity such as ECoG and MEG.

Acknowledgements

This work was supported by the EPSRC through Grant GR/T09903/01. The authors thank to Dr. Zygierewicz and Dr. Durka for helping implementing their algorithm and for useful comments about the proposed algorithm.

References

American Clinical Neurophysiology Society. Guideline 5. Guidelines for standard electrode position nomenclature. J Clin Neurophysiol 2006; 23(2):107–110.

Benjamin Y, Yekuteli Y. The control of the false discovery rate under dependency. Ann Stat 2001;29:1165–88.

Biosemi ActiveTwo System. Frequently asked questions. <http://www.biosemi.com/faq/>; 2007 [11.7.07].

Blankertz B, Dornhege G, Krauledat M, Muller KR, Kunzmann V, Losch F, et al. The Berlin brain–computer interface: EEG-based communication without subject training. IEEE Trans Neural Syst Rehabil Eng 2006;14(2):147–52.

Box GEP, Cox DR. An analysis of transformations. J Roy Stat Soc 1964;2:211–52.

Crone NE, Diana LM, Gordon B, Sieracki JM, Wilson MT, Uematsu S, et al. Functional,mapping of human sensorimotor cortex with electrocorticographic spectral analysis. I Alpha and beta event-related desynchronisation. Brain 1998a;121:2271–99.

Crone NE, Miglioretti DL, Gordon B, Lesser RP. Functional mapping of human sensorimotor cortex with electrocorticographic spectral analysis. II. Event-related synchronization in the gamma band. Brain 1998b;121(Pt 12):2301–15.

Curran E, Sykacek P, Stokes M, Roberts SJ, Penny W, Johnsrude I, et al. Cognitive tasks for driving a brain–computer interfacing system: a pilot study. IEEE Trans Neural Syst Rehabil Eng 2004;12(1):48–54.

Durka PJ. Time–frequency microstructure and statistical significance of ERD and ERS. Prog Brain Res 2006;159:121–33.

Durka PJ, Ircha D, Neuper C, Pfurtscheller G. Time–frequency microstructure of event-related electro-encephalogram desynchronisation and synchronisation. Med Biol Eng Comput 2001;39(3):315–21.

Georgopolos AP, Kalaska JF, Caminiti R, Massey JT. On the relations between the direction of two-dimensional arm movements and cell discharge in primate motor cortex. J Neurosci 1982;2:1527.

Graimann B, Huggins JE, Levine SP, Pfurtscheller G. Visualization of significant ERD/ERS patterns in multichannel EEG and ECoG data. Clin Neurophysiol 2002;113(1):43–7.

Graimann B, Pfurtscheller G. Quantification and visualisation of event-related changes in oscillatory brain activity in the time–frequency domain. Prog Brain Res 2006;159:79–97.

Hermens HJ, Freriks B. 1999. Surface electro-myography for non-invasive assessment of muscles recommendation European concerted action in the Biomedical Health and Research Programme (Biomed II) of the European Union. Recommendation for the recording of SEMG signal (CD-ROM).

Hermens HJ, Freriks B. Surface electro-myography for non-invasive assessment of muscles recommendation. European concerted action in the Biomedical Health and Research Programme (Biomed II) of the European Union. Signal Processing Recommendation. (CD-ROM) 1999.

Hjort B. An online transformation of EEG scalp potentials into orthogonal source derivations. Electroenceph Clin Neurophys 1975;39:526–30.

Hopf JM, Mangum GR. Shifting visual attention in space: an electrophysiological analysis using high spatial resolution mapping. Clin Neurophysiol 2000;111:1241–57.

Kakei S, Hoffman DS, Strick PL. Muscle and movement representations in the primary motor cortex. Science 1999;285(5436):2136–9.

Kauhanen L, Nykopp T, Lehtonen J, Jylanki P, Heikkonen J, Rantanen P, et al. EEG and MEG brain–computer interface for tetraplegic patients. IEEE Trans Neural Syst Rehabil Eng 2006;14(2):190–3.

Krause CM. Cognition- and memory-related ERD/ERS responses in the auditory stimulus modality. Prog Brain Res 2006;159:197–207.

Lebedev MA, Carmena JM, O'Doherty JE, Zacksenhouse M, Henriquez CS, Principe JC, et al. Cortical ensemble adaptation to represent velocity of an artificial actuator controlled by a brain–machine interface. J Neurosci 2005;25(19):4681–93.

Leocani L, Magnani G, Comi G. Event related desynchronisation during execution, imagination and withholding of movement. In: Pfurtscheller G, Lopes da Silva FH, editors. Handbook of Electroencephalography and Clinical Neurophysiology. Amsterdam: Elsevier 1999;6:291–302.

Makeig S. Auditory event-related dynamics of the EEG spectrum and effects of exposure to tones. Electroenceph Clin Neurophysiol 1993;86(4):283–93.

Mallat S, Zhang Z. Matching pursuit with time–frequency dictionaries. IEEE Trans Signal Process 1993;41:3397–415.

MettingVanRijn AC, Peper A, Grimbergen CA. High quality recording of bioelectric events. I: interference reduction, theory and practice. Med Biol Eng Comput 1990;28:389–97.

Munk F. Introduction to joint time–frequency analysis. Compendium for the course. 1st ed. Aalborg: Aalborg University, 2000:69–80.

Neubauer AC, Fink A, Grabner RH. Sensitivity of alpha band ERD to individual differences in cognition. Prog Brain Res 2006;159:167–78.

Neuper C, Scherer R, Reiner M, Pfurtscheller G. Imagery of motor actions: differential effects of kinesthetic and visual-motor mode of imagery of single-trial EEG. Cogn Brain Res 2005;25:668–77.

Neuper C, Wortz M, Pfurtscheller G. ERD/ERS patterns reflecting sensorimotor activation and deactivation. Prog Brain Res 2006;159:211–22.

Onton J, Makeig S. Information-based modeling of event-related brain dynamics. Prog Brain Res 2006;159:99–134.

Pfurtscheller G, Aranibar A. Event-related cortical desynchronization detected by power measurements of scalp EEG. Electroenceph Clin Neurophysiol 1977;42(6):817–26.

Pfurtscheller G. Quantification of ERD and ERS in the time domain. In: Pfurtscheller G, Lopes da Silva FH, editors. Handbook of Electroencephalography and Clinical Neurophysiology. Amsterdam: Elsevier, 1999;6:89–106.

Pfurtscheller G, Lopes da Silva FH. Event-related EEG/MEG synchronization and desynchronization: basic principles. Clin Neurophysiol 1999;110(11):1842–57.

Pfurtscheller G, Pichler-Zalaudek K, Neuper C. ERD and ERS in voluntary movement of different limbs. In: Pfurtscheller G, Lopes da Silva FH, editors. Handbook of Electroencephalography and Clinical Neurophysiology. Amsterdam: Elsevier, 1999;6:245–68.

Pfurtscheller G, Neuper C. Motor imagery and direct brain–computer communication. Proc IEEE 2001;89:1123–34.

Qian S, Chen D. Joint time–frequency analysis: Methods and applications. Prentice Hall; 1996.

Tallon-Baudry C, Bertrand O. Oscillatory gamma activity in humans and its role in object representation. Trends Cogn Sci 1999;3(4):151–62.

Talsma D, Woldorff MG. Methods for the estimation and removal of artifacts and overlap in ERP waveforms. In: Handy TC, editor. Event-related potentials. A method handbook. The MIT Press, 2005:115–49.

Townsend G, Graimann B, Pfurtscheller G. A comparison of common spatial patterns with complex band power features in a four-class BCI experiment. IEEE Trans Biomed Eng 2006;53(4):642–51.

Vidaurre C, Schloegl A, Cabeza R, Scherer R, Pfurtscheller G. A fully on-line adaptive BCI. IEEE Trans Biomed Eng 2006;53:1214–9.

Vuckovic A, Sepulveda F. EEG single trial classification of four classes of imaginary wrist movements based on Gabor coefficients. In: Proc. 3rd Int BCI Workshop. Graz. Austria 2006:26–7.

Zygierewicz J, Durka PJ, Klekowicz H, Franaszczuk PJ, Crone NE. Computationally efficient approaches to calculating significant ERD/ERS changes in the time–frequency plane. J Neurosci Methods 2005;145(1–2):267–76.

Wolpaw JR, Birbaumer N, McFarland DJ, Pfurtscheller G, Vaughan TM. Brain–computer interfaces for communication and control. Clin Neurophysiol 2002;113(6):767–91.